



Shear Resistance Behavior of Exterior Beam-Column Joint with Steel Fiber Reinforced Concrete

Charu Gupta¹, Siva Chidambaram Rajendran²(✉), and A. B. Danie Roy¹

¹ Department of Civil Engineering, Thapar Institute of Engineering and Technology, Patiala 147004, India

² CSIR-Central Building Research Institute, Roorkee 247667, India
krsinelastic@gmail.com, schidambaram@cbri.res.in

Abstract. The beam-column joint in the reinforced concrete (RC) framed structure acts as the critical part in the structure, which participates to carries large vertical and horizontal shear forces during the seismic event. The past earthquake damages demonstrate the importance of shear resistance and energy dissipation capacity of beam-column joints. The conventional transverse reinforcement detailing at the potential hinge region improves the shear capacity to a certain extent and the brittle nature of concrete limit the efficiency of the joint. Also, the critical detailing leads to steel congestion and construction difficulty. The employment of discontinuous randomly distributed steel fiber in the concrete (SFRC) offers better post-peak strain in the form of strain-softening which offers better ductility. The use of SFRC in RC elements acts as secondary shear reinforcement in resisting the shear force with improved damage tolerance and energy dissipation. This article presents an experimental study on the cyclic behavior of exterior beam-column joints with different profile steel fiber in different volumes. The joints have been prepared without critical detailing and SFRC has been used only at the joint hinge region. The hysteresis behavior of the joint specimen shows that the SFRC effectively improves the shear carrying capacity of the joint with increased ductility and damage tolerance without the need for closely spaced stirrups at the joint hinge region. The shear strength enhancement observed in the study has been validated using the available models.

Keywords: Beam-column joint · Steel fibers · Shear failure · Energy dissipation

1 Introduction

The combined forces from beams and columns increase the shear demand of the beam-column of the reinforced concrete (RC) frame structure and make it a vulnerable part when subjected to seismic force. Earthquake reconnaissance survey displays the importance of beam-column joint design and detailing to make more damage tolerant and to restrict the shear failure. In order to improve the efficiency of the joint code of practices are high recommend a higher percentage of transverse stirrups at the joint plastic hinge.

This may lead to reinforcement congestion and construction difficulties during casting. In order to overcome these issues randomly distributed short steel fibers in concrete (SFRC) are emerging in construction. The use of discrete fibers in concrete adds tensile strength and post-peak strain which improves the toughness characteristics of the SFRC. The discrete fibers in the concretes are effectively transferred the forces across the cracks through their crack-bridging capacity. The resistance to early crack formation and the bridging effect during the large deformation improves the damage tolerance and restricts the spalling of concrete. In the past few decades application of SFRC is intensely varied and widespread consequently making it hard to classify in assorted categories. It has been used for applications such as airport pavements, shotcrete, tunnel linings, etc. The use of SFRC in the beam-column joint region improves the shear strength of the joint with an optimum amount of stirrups (Chidambaram et al. 2015 and 2020). It acts as secondary shear reinforcement and eliminates the need for closely spaced stirrups (Chidambaram et al. 2019). The crack resistance mechanism improves the stiffness at an initial stage and also offers better stiffness retention during the inelastic rotation. The energy dissipation and damping property of SFRC are highly commendable in resisting seismic forces. The ductile behavior of beam-column joints is primarily governed by the design and detailing, the use of SFRC reduces the need for closely spaced transverse reinforcement and acts as micro-level shear reinforcement, and possesses better elastic and inelastic behavior compared to the brittle concrete.

2 Literature Review

Jiuru et al. (1992) conducted an experimental study using five exterior beam-column joints employed with SFRC and tested under reversed cyclic loading. The studied parameters were the reinforcement ratio, stirrups ratio, and development length in the joint of the beam. Results obtained specify an increase in shear strength, ductility, and energy-dissipation capacities. Mustafa Gencoglu (2007) experimented with the use of SFRC and stirrup together in the joints with different fiber volumes. The test results were evaluated in terms of the load-carrying capacity, shear strength, ductility, energy dissipated, and the recovered elastic energy. It shows that the SFRC in the joint region improves the strength, energy dissipation and improves the flexural rigidities of plastic hinge regions. Mustafa et al. (2002) conducted the study using the four beam-column full-scale joints under reversed cyclic loading and the test was evaluated with respect to strength, energy absorption, and damage. The test result shows that with the decrease in the transverse reinforcement in the joint and confinement area of the beam and the column, there could be an improvement in strength capacity and ductility with the use of SFRC. Kwon et al. (2011) conducted the investigation on the outcomes of SFRC in the RC beam-column exterior joint region and the possibility of replacing some joint area transverse reinforcement. The test parameters considered were the ratio of steel fibers volumes i.e., (0%, 1%, and 1.5%) and amount of confinement in the joint region. Therefore, the test results indicated that SFRC had improved the maximum capacity, bond condition, shear strength, and energy dissipation capacity. Patel et al. (2013) studied the application of SFRC beyond the increased hoop spacing of lateral ties in accordance to impart ductility in a beam-column joint. Testing was done under reversed cyclic loading

for six one-third-scale exterior beam-column joints. Test results showed improvement in the connection behavior with respect to strength, energy dissipation, specific damping capacity, displacement ductility, and stiffness. Craig et al. (1984) conducted the experimental study using ten beam-column specimens with half of these specimens contains steel hooked end fibers with 1.5% by volume of concrete. The test result showed that Steel hooked end fiber provided improvement in energy dissipation capacity, ductility, bond, better confinement of the concrete, higher moment capacity, and shear strength.

3 Research Significance

Various experimental studies were carried out to determine the effectiveness of SFRC in joint shear resistance and observed that the use of SFRC improves strength and ductility. Few shear strength models have been proposed to estimate the shear resistance capacity of SFRC joints. These models consider the volumetric content of fibers, the strength of concrete, axial load ratio, etc. This study aims to propose a simplified shear strength model to estimate the shear resistance capacity of SFRC joints and to validate the model using the experimental outcome and the literature data available.

4 Experimental Program

This experimental research examines the influence of the hooked end steel fiber with an optimum amount of stirrups on the shear capacity and ductile performance of beam-column joints.

4.1 Material and Test Setup

Cementitious material as Ordinary Portland Cement (OPC) that contains the coarse aggregate of size 20 mm. Steel fiber with a Hooked end of 35 mm length and a diameter of 0.60 mm (aspect ratio = 60) and 1100 MPa as nominal tensile strength is considered to develop SFRC. Several standard sizes of 100 mm × 200 mm cylinder specimens were cast and tested in a 1000 KN universal testing machine (CTM) for determining the compressive strength of the specimens (Table 1).

Table 1. Compressive strength of various specimens

Samples	Description	Fiber content (%)	Cylinder compressive strength (MPa)
JS1	Conventional	-	20
JS2	End-Hooked	1	36.66

4.2 Test Setup of Beam-Column Joint

Two exterior beam-column joint specimens with similar reinforcement detailing as shown in Fig. 1 are used in this study with a development length (l_d) of 400 mm. The joint specimens are tested under compression cyclic loading using FEMA 461 (2007). Table 2 presents the typical details of beam-column joints. All the joint specimens are tested under displacement-controlled reverse cyclic loading to evaluate the hysteresis behavior of different SFRC specimens (Fig. 2).

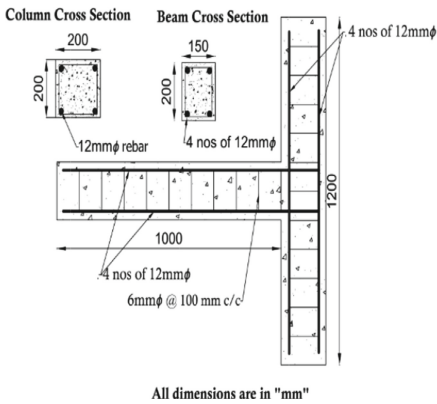


Fig. 1. Typical reinforcement detail of joint specimens.

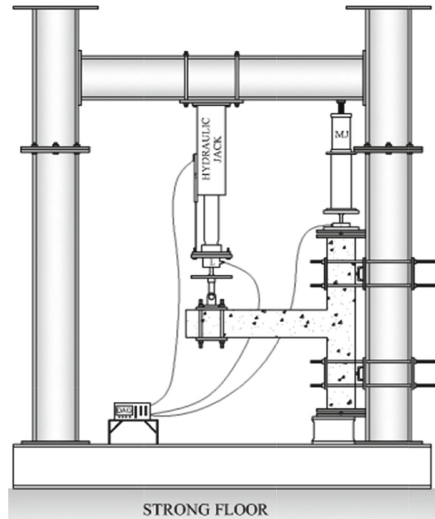


Fig. 2. Test setup of specimen.

Table 2. Detail of exterior beam-column joint specimens with SFRC

Specimens	Transverse reinforcement	Type of joint	Beam reinforcement	Column reinforcement
JS1	$\text{Ø}6$ mm@100 mm C/C	Conventional	All specimens are reinforced with 4 nos. of 12 mm Ø at the top and bottom	All specimens are reinforced with 4 nos. of 12 mm Ø
JS2	$\text{Ø}6$ mm@100 mm C/C	End-Hooked		

5 Results and Discussions

5.1 Failure Mode and Crack Propagation

The brittle nature of conventional concrete fails to restrict the formation of the early crack, which leads to longitudinal reinforcement slip and diagonal shear cracks formation.

Figure 4 shows the crack pattern of JS1 and JS2. Initially, flexural cracks were noticed in JS1 whereas the absence of closely spaced stirrups and diagonal cracks formation during inelastic rotation exhibits shear failure as shown in Fig. 3 (a, b). The presence of steel fiber in JS2 restricts the early crack formation and allows the plastic hinge to rotate with multiple micro-cracks as shown in Fig. 3 (c, d). The final failure was noticed at the joint interface with rebar yielding and there was no sign of shear cracks at the joint region. It proves the efficacy of the SFRC in resisting the joint shear with better damage resistance with an optimum amount of stirrups.



(a)



(b)



(c)



(d)

Fig. 3. (a,b) Crack pattern for JS1 and (c,d) Crack pattern for JS2.

5.2 Hysteresis Behavior

Figure 4 shows the hysteresis behavior of joint specimens. The yield load of JS1 is 40% lower than JS2 as a result of early joint shear failure. The peak load of JS 1 is

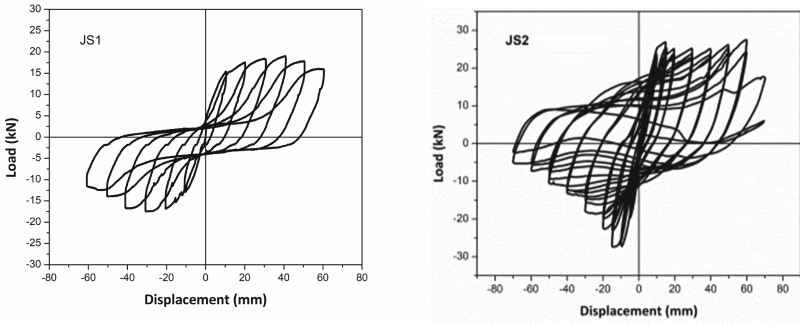


Fig. 4. Hysteresis curves of different samples.

19.5 kN whereas it is 27 kN for JS2. Hysteresis curve of JS 1 shows load drop after 40 mm displacement (positive push) whereas there is no sign of load drop till 60 mm displacement in specimen JS2. The sudden load drop after 60 mm displacement is due to the rebar rupture observed at the joint interface. The pinched loop in JS1 is primarily because of shear cracks and reinforcement slippage from the joint whereas the presence of SFRC in JS2 shows an enlarged loop compared to JS1. The post peaks strength degradation of JS 2 is gradual than JS1 and the same can be understood from the envelope curve as shown in Fig. 5(a) yielding occurred.

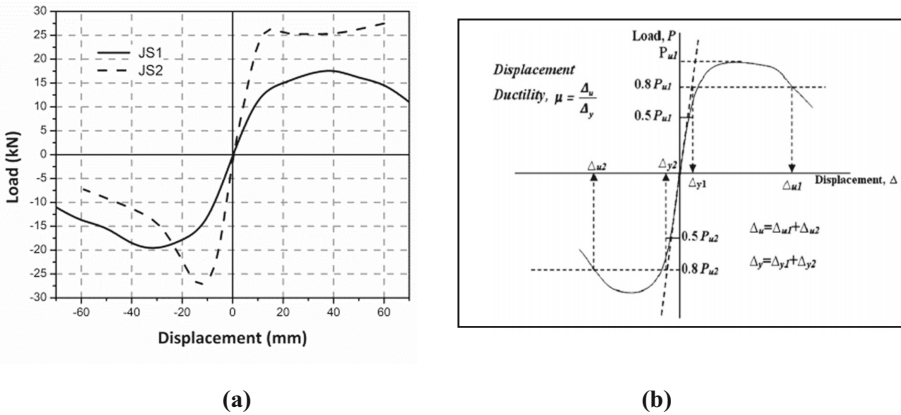


Fig. 5. Load-displacement envelopes over displacement.

5.3 Stiffness Degradation

Figure 6 and 7 shows the positive stiffness degradation and negative stiffness degradation over drift respectively. The initial and secant tangent is used to measure the initial and post-yield stiffness of the specimens Chidambaram et al. (2020). The initial level of crack resistance offered by steel fibers in JS2 shows 1.5 times higher yield stiffness compared to JS1. Figure 6 shows the enhanced stiffness retention capacity of JS2 over JS1. The observed stiffness at failure is 45% higher than JS1, which authenticates the efficacy of the steel fibers confinement action in providing inelastic stiffness retention. JS1 stiffness is 2.5 whereas JS2 Stiffness goes from 2.5 to 3.75 in positive stiffness degradation and in negative stiffness degradation the stiffness goes from 3 to 4 with an increase in drift ratio. The yield stiffness is defined from Fig. 5 (a) Chidambaram et al. (2015).

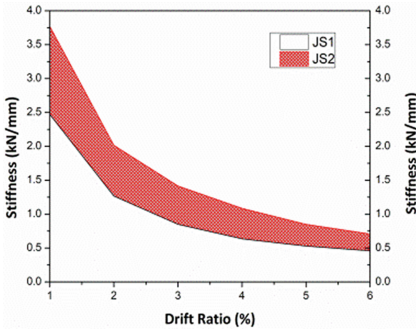


Fig. 6. Positive stiffness degradation over drift.

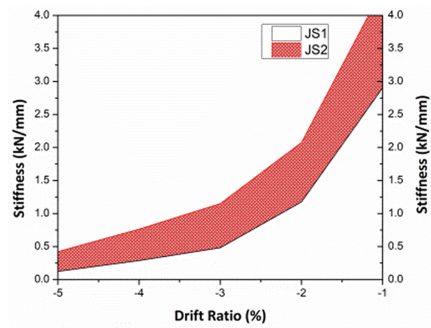


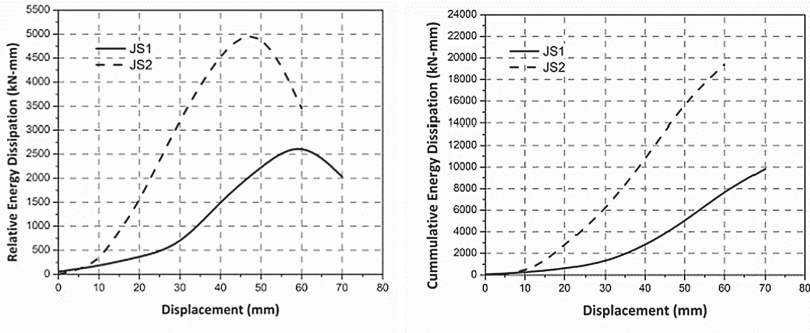
Fig. 7. Negative stiffness degradation over drift.

5.4 Energy Dissipation and Damping

The energy dissipation of a structural element is a prime source of ductility estimation. The ratio between the observed and dissipated energy plays a vital role in damage tolerance. The area enclosed by the loop is used to estimate the dissipated energy and Equation I is used to estimating the damping coefficient. Relative (RED) and cumulative energy dissipation (CED) are calculated and shown in Fig. 8 (a) and 8 (b) respectively. The JS2 shows 2.375 times higher CED than JS 1 at 60 mm displacement and a similar trend has been observed with RED.

The equivalent damping coefficient is measured using the ratio between the strain energy and dissipated energy. Figure 9 shows that the JS1 and JS2 have almost similar damping capacity at yield whereas the JS2 possesses better and improved damping capacity over JS 1 during a higher drift ratio. The yield point is a starting point as the ductility value starts from 1 and The JS 2 possesses 1.7 times higher damping at 4% drift and it is 1.37 times at 5% drift ratio compared to JS1. It proves that the ability of SFRC in offering inherent structural damping capacity of joints.

$$\xi_{eq} = \frac{1}{2\pi} \left\{ \frac{\text{area of loop}}{\text{area of triangle}} \right\} \tag{1}$$



(a) Relative Energy Dissipation (b) Cumulative Energy Dissipation

Fig. 8. Energy dissipation versus displacement.

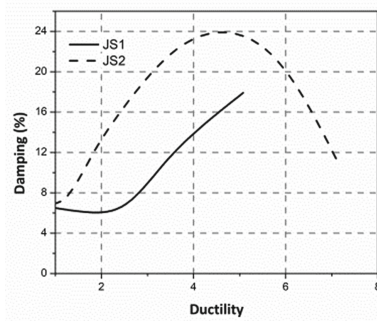


Fig. 9. Equivalent damping coefficients over ductility.

5.5 Damage Index and Pinching Width Ratio

The damage tolerance of the beam-column joint is measured using the modified park and damage index as per Eq. 2. Also the pinching width ratio is used to correlate the damage tolerance. Park et al. (1987)

$$D = \frac{\delta_m}{\delta_u} + \frac{\beta}{F_y \delta_u} \int dE \tag{2}$$

where “ δ_M ” is the demand of maximum displacement under cyclic loading; “ δ_U ” is the capacity of ultimate displacement. The integral part is the amount of energy dissipation under cyclic loading and “ F_y ” is the yield strength and “ β ” is the strength degradation, and its value is “0.1” for RC structure Isabelle Villemure (1993). Figure 10 shows the DI measured versus ductility. It shows that the JS 2 posses one level higher damage tolerance due to the crack bridging effect, absence of spalling of concrete, and absence of shear failure due to the existence of steel fiber.

During reloading after unloading, the pinching behavior was observed in the hysteresis response of the specimen which was subjected to reverse loading that majorly

leads to large stiffness reduction. When concrete loses a considerable amount of its compression bearing capacity that leads to a significant reduction in its flexural stiffness, and occurrence of stiffness reduction. The pinching width ratio is defined as pinching width in the actual force-drift ratio curve (P_a) divided by pinching width in an idealized curve (P_i) Alavi-Dehkordi (2019). Figure 11 shows the effect of the brittleness of conventional concrete and its inefficiency in stiffness retention. JS2 shows a two-fold wider loop compared to JS 1 at a 5% drift ratio whereas it is 3.3 fold higher at failure drift. Hence, it proves that the occurrence of steel fiber work at the micro and macro level in resisting the crack growth, and as a result, better stiffness retention capacity is established which significantly reduced the pinching in the hysteresis curve.

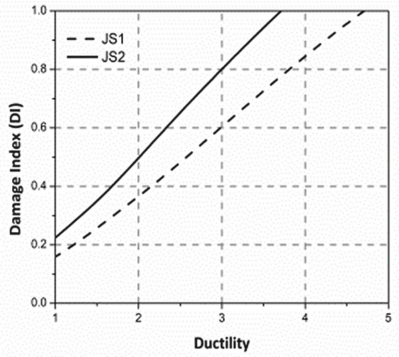


Fig. 10. Damage index over ductility.

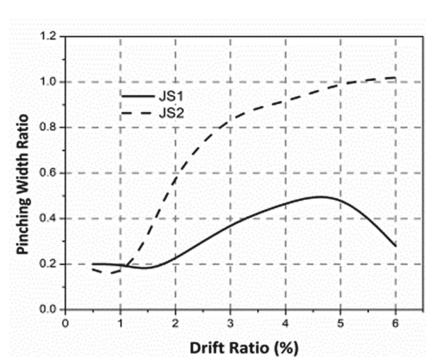


Fig. 11. Pinching width ratio versus drift.

6 Calculation of Joint Shear Strength

The ultimate shear strength of an SFRC joint can be calculated by using concrete as shown in Eq. (3), by using fiber shown in Eq. (4), and with the use of stirrup resistance shown in Eq. (5). As mentioned in Table 3, According to codal provision the shear strength was evaluated but it’s only applicable for conventional concrete not for fibers. So to evaluate the ultimate shear strength of SFRC joint, one of the equation was proposed by Jiuru et al. (1992) and Kim et al. (2011) as follows,

$$V_j = V_c + V_f + V_s \tag{3}$$

Where,

V_j = Ultimate shear strength of joint.

V_c = Shear carried by concrete

$$V_c = 0.1 \left(1 + \frac{N}{b_c h_c f_c} \right) b_j h_j f_c' \tag{4}$$

V_f = Shear carried by fiber

$$V_f = 2 \frac{l_f}{d_f} v_f b_j h_j \tag{5}$$

V_s = Shear carried by joint stirrups

$$V_s = f_y \frac{A_{sh}}{S} (h_o - a'_s) \tag{6}$$

Where,

N : Axial load, f'_c : Concrete compressive cylinder strength, h_c : depth of column, b_c : width of the column, f_c : Concrete compressive strength, b_j : effective width of joint transverse to the direction of shear, h_j : effective depth of joint parallel to the direction of shear, l_f : Length of fiber, d_f : Diameter of fiber, f_y : yield strength, A_{sh} : area of shear reinforcement within distance S , h_o : effective depth of the beam, S : spacing of stirrups, a'_s : distance from extreme compressive fiber to centroid of compressive reinforcement.

Table 3. Comparison of shear strength using different models

Sample	V_f	V_{jh} calculated	ACI 318–14	IS 13920:2016
	(%)	kN	kN	kN
JS1	-	76.76	178.88	178.88
JS2	1	134.33	242.19	242.19

7 Comparison of Shear Strength

The shear strength of the Beam-Column RC joint can be determined with two codes of seismic design as shown in Table 4. to calculate the joint shear strength, Concrete compressive strength (f_c), and the common region of effective (A_{ej}) has been considered. The ACI 318 code considers the modification factors (ϕ) for concrete of two types i.e. 1.00 for concrete of normal weight, and 0.75 for concrete of lightweight. In IS 13920:2016 and ACI 318–14 the (λ) represents the effect of transverse reinforcement of the beams to the joints which are equal to 1. The code predicted shear strength of the joint is compared with considering the area ratio approach in the experimental database as shown in Fig. 12, with ACI and IS Code and with ACI and IS modification factor.

Table 4. Joint shear strength according to codes for conventional concrete

	Codes	Joint shear strength equation
1	ACI 318-14	$V_{jh}^{ACI} = \lambda \phi \sqrt{f_c} A_j$
2	IS 13920:2016	$V_{jh}^{IS} = \lambda \sqrt{f_c} A_j$

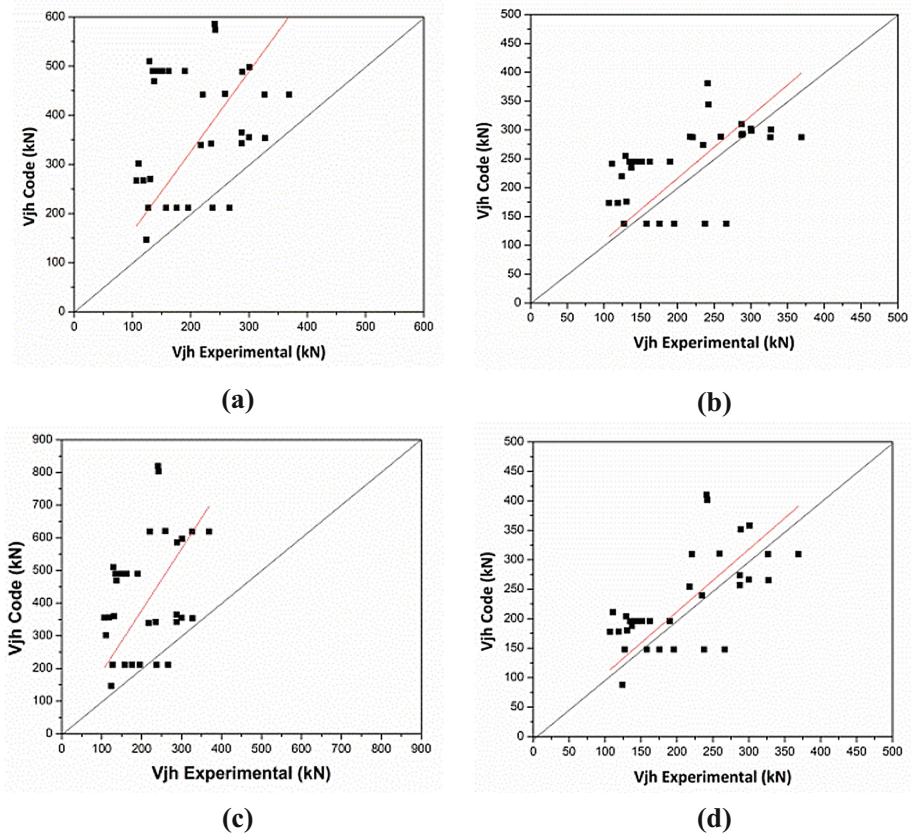


Fig. 12. The code predicted shear strength of joint compared with the consideration of the area ratio approach, for (a) ACI 318–2014,(b) ACI with modification, (c) IS 13920:2016, and (d) IS with modification.

The coefficient of variance of ACI and IS are 0.42 and 0.49 with an average of 0.61 and 0.56 respectively. The co-variance of the modified ACI and IS equation proposed are 0.59 and 0.38 with an average of 0.92 and 0.90. The R^2 of ACI and IS are 0.83 and 0.84 respectively. The R^2 of ACI and IS with modified factors are 0.92 and 0.91 respectively. The ratio of the slope of R^2 for ACI and IS are 1.88 and 1.62 respectively, whereas for ACI and IS with modified factor are 1.05 and 1.07 respectively. The shear strength with the modified factors in the area ratio approach can calculate the joint shear strength with more precision for SFRC. It has been validated using the experimental data and using the literature review data as per the details given in the appendix-A.

8 Conclusion

1. Under cyclic loading, the hysteresis behavior of the JS2 specimen demonstrates a considerable rise in pre and post-peak behavior of the external beam-column joint. the hysteresis damping of the JS2 specimen ranges from 6 to 24% , owing to improve results at a ductility level of around 5 and gradual losses in the hysteresis damping as ductility rises from 5 to 7. However, in the JS1 damping hysteresis specimen goes from 6 to 18% over the maximum ductility level of 5.
2. Figure 12 shows the comparison between the codal provisions of ACI 318–2014 and IS 13920:2016 and with modified factors of ACI 318–2014 and IS 13920:2016 based on an approach to the ratio of the area with the experimental results. The code predicted joint shear strength with modified factors shows more accuracy compared with code recommendations.
3. The failure mechanism and pattern of cracking of JS2 specimen marks uniform energy dissipation with a wide crack in the joints. This forms a horizontal crack at the joint intersection of the beam column along with a small shear crack that increases when deformation increases while in JS1 specimens it shows a diagonal shear crack failure in the joint area.
4. The joint shear strength of the SFRC joint has been calculated using the codal provisions meant for conventional concrete which estimates the joint shear with an average of 0.56 and 0.61. The slope of the linear fit of ACI and IS is 1.88 and 1.52 respectively. The proposed modified equation has been used to estimate the joint shear of the SFRC joint and observed an average value of 0.92 and 0.91 respectively. Similarly, the slope of the modified equation linear fit is 1.05 and 1.07 respectively. Its shows the efficacy of the proposed modification in estimating the joint shear capacity of the SFRC joint. The equation proposed by Jiuru et al. (1992) has three parts such as the contribution of concrete, stirrups, and fiber. In which the physical meaning of fiber contribution is wrong and the outcome is in sq. mm.
5. PWR calculated for JS1 and JS2 specimens show that the use of SFRC improves the energy dissipation by increasing the loop area. The measure PWR of JS 2 is 230% higher than JS1. It signifies the role of SFRC in resisting the shear force with enhanced ductility.

Appendix-A

S. No	ID	Vf	Exp V/jh	ACI-138-14	VjhExp/Vjh ACI	Modified factor of ACI	ACI modifiedV/jh	VjhExp/Vjh ACI modified	IS:13920-2016	VjhExp/Vjh IS	Modified factor of IS	IS modifiedV/jh	VjhExp/Vjh IS modified
Juna et al. (1992)													
1	SF1	1.2	326.74	618.83	0.52	0.5	309.41	1.05	442.02	0.73	0.65	287.31	1.13
	SF2	1.5	368.94	618.83	0.59	0.5	309.41	1.19	442.02	0.83	0.65	287.31	1.28
	SF3	1.5	259.15	620.77	0.41	0.5	310.38	0.83	443.41	0.58	0.65	288.21	0.89
	SF5	1.5	220.84	618.83	0.35	0.5	309.41	0.71	442.02	0.49	0.65	287.31	0.76
Wang et al. (2018)													
2	EJ1	1.3	287.5	342.84	0.83	0.75	257.13	1.11	342.84	0.83	0.85	291.41	0.98
	EJ2	1.3	287.5	364.76	0.78	0.75	273.57	1.05	364.76	0.78	0.85	310.05	0.92
	EJ3	1.3	300	354.98	0.84	0.75	266.24	1.12	354.98	0.84	0.85	301.73	0.99
	EJ4	1.3	217.5	339.12	0.64	0.75	254.34	0.85	339.12	0.64	0.85	288.25	0.75
	EJ5	1.3	327.5	353.50	0.92	0.75	265.12	1.23	353.50	0.92	0.85	300.47	1.08
Oinam et al. (2018)													
3	SFRC-0.75	0.75	301	596.99	0.50	0.6	358.19	0.84	497.49	0.60	0.6	298.49	1.00
	SFRC-1.0(1)	1	288.76	586.03	0.49	0.6	351.62	0.82	488.36	0.59	0.6	293.01	0.98
	SFRC-1.0(2)	1	242.26	803.28	0.30	0.5	401.64	0.60	573.77	0.42	0.6	344.26	0.70
	SFRC-1.5	1.5	241.16	819.92	0.29	0.5	409.96	0.58	585.66	0.41	0.65	380.68	0.63
Patel et al. (2013)													
4	ND	1.5	127.29	211.23	0.60	0.7	147.86	0.86	211.23	0.60	0.65	137.30	0.92
	NDS2	1.5	157.89	211.23	0.74	0.7	147.86	1.06	211.23	0.74	0.65	137.30	1.15
	D	1.5	175.81	211.23	0.83	0.7	147.86	1.18	211.23	0.83	0.65	137.30	1.28
	DS1S2	1.5	237.61	211.23	1.12	0.7	147.86	1.60	211.23	1.12	0.65	137.30	1.73
	DS2S2	1.5	266.48	211.23	1.26	0.7	147.86	1.80	211.23	1.26	0.65	137.30	1.94
	DS3S2	1.5	195.60	211.23	0.92	0.7	147.86	1.32	211.23	0.92	0.65	137.30	1.42
Ganesan et al. (2007)													
5	F2HPr	0.5	106.93	355.52	0.30	0.5	177.76	0.60	266.64	0.40	0.65	173.31	0.61
	F3HPr	0.75	118.84	355.97	0.33	0.5	177.98	0.66	266.98	0.44	0.65	173.53	0.68
	F4HPr	1	130.71	360	0.36	0.5	180	0.72	270	0.48	0.65	175.5	0.74
Mustafa Gencoglu (2007)													
6	SFRC3hstr	1	189.94	489.89	0.38	0.4	195.95	0.96	489.89	0.38	0.5	244.94	0.77

(continued)

(continued)

S. No	ID	Vf	Exp Vjh	ACI-138-14	VjhExp/Vjh ACI	Modified factor of ACI	ACI modified Vjh	VjhExp/Vjh ACI modified	IS:13920-2016	VjhExp/Vjh IS	Modified factor of IS	IS modified Vjh	VjhExp/Vjh IS modified
	SFRC2h	1	162.41	489.89	0.33	0.4	195.95	0.82	489.89	0.33	0.5	244.94	0.66
	SFRChstr	1	134.88	489.89	0.27	0.4	195.95	0.68	489.89	0.27	0.5	244.94	0.55
	SFRCh	2	143.14	489.89	0.29	0.4	195.95	0.73	489.89	0.29	0.5	244.94	0.58
	SFRC(1/2hstr	1	151.40	489.89	0.30	0.4	195.95	0.77	489.89	0.30	0.5	244.94	0.61
Gençoglu et al. (2002)													
7	# 3 SFRC	1	137.25	469.04	0.29	0.4	187.61	0.73	469.04	0.29	0.5	234.52	0.58
	# 4 SFRC	1	129.29	509.90	0.25	0.4	203.96	0.63	509.90	0.25	0.5	254.95	0.50
Bharti et al. (2017)													
8	JS4	1	124.08	146.35	0.84	0.6	87.81	1.41	146.35	0.84	1.5	219.53	0.56
Shakya et al. (2012)													
9	BCI-1.0	1	110.78	301.68	0.36	0.7	211.18	0.52	301.68	0.36	0.8	241.35	0.45
	BCI-1.5	1.5	235.10	342.32	0.68	0.7	239.62	0.98	342.32	0.68	0.8	273.86	0.85
				Avg	0.56		Avg	0.94	Avg	0.61		Avg	0.90
				Cov	0.49		Cov	0.32	Cov	0.42		Cov	0.38

References

- Alavi-Dehkordi, S., Mostofinejad, D., Alaei, P.: Effects of high-strength reinforcing bars and concrete on seismic behavior of RC beam-column joints. *Eng. Struct.* **183**, 702–719 (2019). <https://doi.org/10.1016/j.engstruct.2019.01.019>
- ACI Committee 318: Building code requirements for structural concrete (ACI 318–14) and commentary (ACI 318R-14). American Concrete Institute, Farmington Hills (2014)
- Bharti, R., Chidambaram, R.S., Kwatra, N.: Influence of fiber reinforced concrete on plastic behavior on exterior beam column joint under cyclic loading. *Procedia Eng.* **173**, 1122–1129 (2017)
- Chidambaram, R.S., Agarwal, P.: Shear resistance behavior of geogrid-confined RC elements under static and cyclic loading. *Curr. Sci.* **117**(2), 260–271 (2019). (00113891)
- Craig, R.J., Mahadev, S., Patel, C.C., Viteri, M., Kertesz, C.: The behavior of joints using reinforced fibrous concrete. *Spec. Publ.* **81**, 125–168 (1984)
- Chidambaram, R.S., Agarwal, P.: Seismic behavior of hybrid fiber reinforced cementitious composite beam-column joints. *Mater. Des.* **86**, 771–781 (2015)
- Chidambaram, R.S., Agarwal, P.: Seismic resistant behavior of exterior beam-column joint with fiber hybridization. *Indian Concr. J.*, 20–30 (2020)
- FEMA 461: Interim Testing Protocols for Determining the Seismic Performance Characteristics of Structural and Non-structural Components. Federal Emergency Management Agency, Washington, D.C., USA (2007)
- Gencoglu, M.: The effects of stirrups and the extents of regions used SFRC in exterior beam-column joints. *Struct. Eng. Mech.* **27**(2), 223–242 (2007)
- Gençoğlu, M., Eren, İ.: An experimental study on the effect of steel fiber reinforced concrete on the behavior of the exterior beam-column joints subjected to reversal cyclic loading. *Turk. J. Eng. Environ. Sci.* **26**(6), 493–502 (2002)
- Ganesan, N., Indira, P.V., Abraham, R.: Steel fiber reinforced high-performance concrete beam-column joints subjected to cyclic loading. *ISIJ Int. Earthq. Technol.* **44**(3–4), 445–456 (2007)
- IS 13920: Ductile design and detailing of reinforced concrete structures subjected to seismic forces Code of practice, India (2016)
- Villemure, I.: Damage Indices for Reinforced Concrete Frames Evaluation and Correlation (Master of Applied Science Thesis). The University of British Columbia (1993)
- Jiuru, T., Chaobin, H., Kaijian, Y., Yongcheng, Y.: Seismic behavior and shear strength of framed joint using steel-fiber reinforced concrete. *J. Struct. Eng.* **118**(2), 341–358 (1992)
- Kwon, W.H., Kim, W.S., Kang, T.H., Hong, S.G., Kwak, Y.K.: The behavior of steel fiber-reinforced concrete exterior connections under cyclic loads. *J. Korea Concr. Inst.* **23**(6), 711–722 (2011)
- Min-gu, K., Yoon-geun, K., Hyun-gu, K., Seong-geol, H., Woo-seok, K., Woo-hyun, K.: Repeat In a loaded high-strength reinforced concrete beam-column connection a study on the reinforcing effect of steel fibers. *J. Architectural Inst. Korea* **23**(6), 1–12 (2011)
- Oinam, R.M., Kumar, P.C.A., Sahoo, D.R.: Effectiveness of Steel Fiber in External Beam-Column Joints under Cyclic Loading (2018)
- Patel, P.A., Desai, A.K., Desai, J.A.: Evaluation of RC and SFRC exterior beam-column joint under cyclic loading for the reduction in lateral reinforcement of the joint region. *Mag. Concr. Res.* **65**(7), 405–414 (2013)
- Park, Y.J., Ang, A.H., Wen, Y.K.: Damage-limiting aseismic design of buildings. *Earthq. Spectra* **3**(1), 1–26 (1987)
- Shakya, K., Watanabe, K., Matsumoto, K., Niwa, J.: Application of steel fibers in beam-column joints of rigid-framed railway bridges to reduce longitudinal and shear rebars. *Constr. Build. Mater.* **27**(1), 482–489 (2012)
- Wang, D., Ju, Y., Zheng, W., Shen, H.: Seismic behavior and shear bearing capacity of ultra-high-performance fiber-reinforced concrete (UHPFRC) beam-column joints. *Appl. Sci.* **8**(5), 810 (2018)